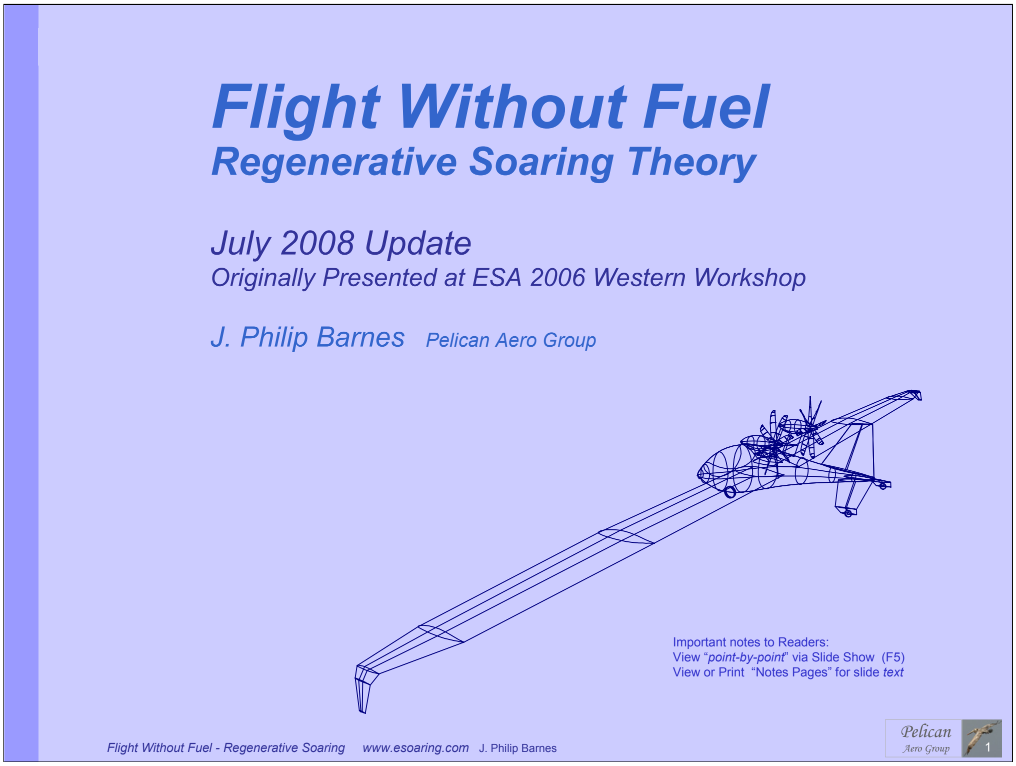

In his 1926 landmark text, "Aerofoil and Airscrew Theory," the great British aerodynamicist Hermann Glauert suggested we "consider the case of a windmill on an aeroplane." Although Glauert offered no specific application thereof, he knew the airborne turbine would one day find important applications.

In 1998, American engineer Paul MacCready introduced "with caution" *regenerative soaring*, where in concept, an aircraft would incorporate energy storage, a propeller, and a wind turbine, or dual-role machine thereof, to propel the aircraft and regenerate stored energy in updrafts.

Today, it is my pleasure to share leading-edge discoveries for this new regime of low-speed flight. Herein we develop an introductory "Regenerative Soaring Theory," and apply it to demonstrate the theoretical feasibility of an entire flight without fuel, including self-contained takeoff, climb, cruise, regeneration, and landing on a full charge.

To begin our study, we first review and expand upon the principles of classical soaring. Then we extend these new methods to evaluate the feasibility of regenerative soaring. We'll show that a regen exhibits both sustainable flight and performance competitive with that of a sailplane, while adding the regen-unique capabilities. Finally, we preview supplemental advantages offered by "solar-augmented" regenerative soaring.

Presentation Contents

This chart has no footnotes

Introduction to Soaring

- Soaring flight is *sustained* by atmospheric motion
  - Repeated “energy cycle” keeps the aircraft aloft
- Requires high efficiency: aero, structural, & systems
- Requires strategy and intelligent maneuvering
- **Classical**: float up in a thermal ~ glide to next thermal
  - High-performance sailplane
- **Dynamic**: “wind profile” ~ upwind climb / d’wind dive
  - Wandering albatross in 20-m boundary layer over flat sea
- **Regenerative**: “windprop” dual-role windmill / prop
  - “Regen” in thermal ~ cruise / pinwheel glide to next thermal
    - Option: “solar-augmented” glide, in lieu of pinwheeling

Interested readers may consult the author’s SAE paper “How Flies the Albatross,” (SAE.org) to understand the flight mechanics of dynamic soaring, as well as the amazing feats of this most marvelous and threatened bird.

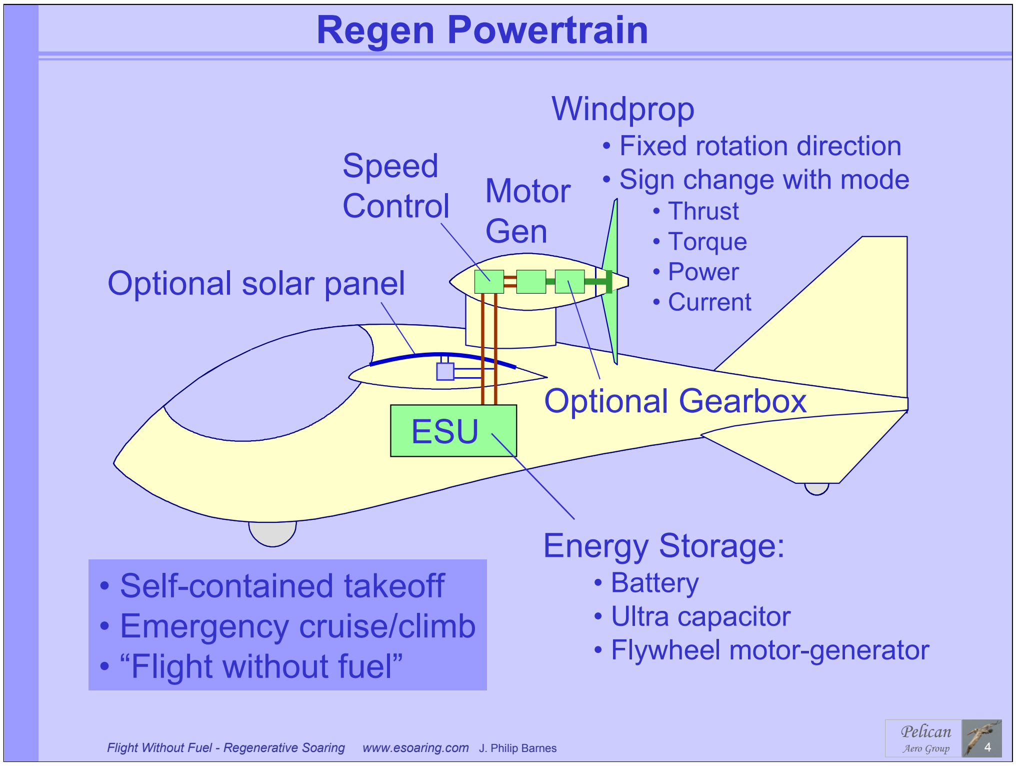

The powertrain of a regenerative aircraft begins with an energy-storage unit, connected with electrical cables to a speed control which conditions the power to and from the motor-generator. A gearbox may be necessary to enable both the motor-generator and windprop to operate over their optimum speed ranges. The system always rotates in the same direction, but when the power mode changes from propeller to turbine, the thrust, torque, power, and current change sign.

We assume 84% efficiency for the powertrain (excluding the windprop), when the system operates in cruise or in high-efficiency regeneration. With 85% "isolated" windprop efficiency, this then obtains 71% "system efficiency" in cruise. System efficiency is considerably lower during climb, where electrical current is much higher, and where windprop efficiency is reduced.

We show here an optional solar panel package for *solar-augmented regenerative soaring*. However, solar power is not included in our regen performance analysis herein.

Elevation and Total Specific Energy

- 3 "*elevations*" to analyze regenerative soaring
  - $z_o \equiv$ Elevation above the ground
  - $z \equiv$ Elevation relative to the "local airmass"
    - relative to ground-based observer for still air
    - relative to balloon-based observer in a thermal
  - $z_t \equiv$ "Total elevation" or "total specific energy"
    - Total system energy *per unit vehicle weight*
      - kinetic + potential + stored

- Corresponding "Climb" rates (m/s) herein:
  - $dz_o / dt \equiv$ climb rate seen by ground-based observer
  - $dz / dt \equiv$ climb rate ($\pm$), relative to local airmass
  - $dz_t / dt \equiv$ Rate of change of total specific energy

This chart has no footnotes

Presentation Contents

This chart has no footnotes

Characteristics of a Thermal

- Rising column of air ~ 1^{o}C warmer than ambient
- 20-min lifetime; grows with square root of time
- Updraft core at about 25% of thermal height
- Low-level: fed from the side ~ cylindrical shape
- Mid-level: fed from above & sides ~ conical shape

Approximate thermal model herein:

- Hybrid of data from Scorer, Carmichael, & Allen
    - Thermal envelope, Radial decay, Core location
- “Static & mature” ~ 4-km height, 5-m/s core
- Assumed to support 16-min of thermalling

This chart has no footnotes

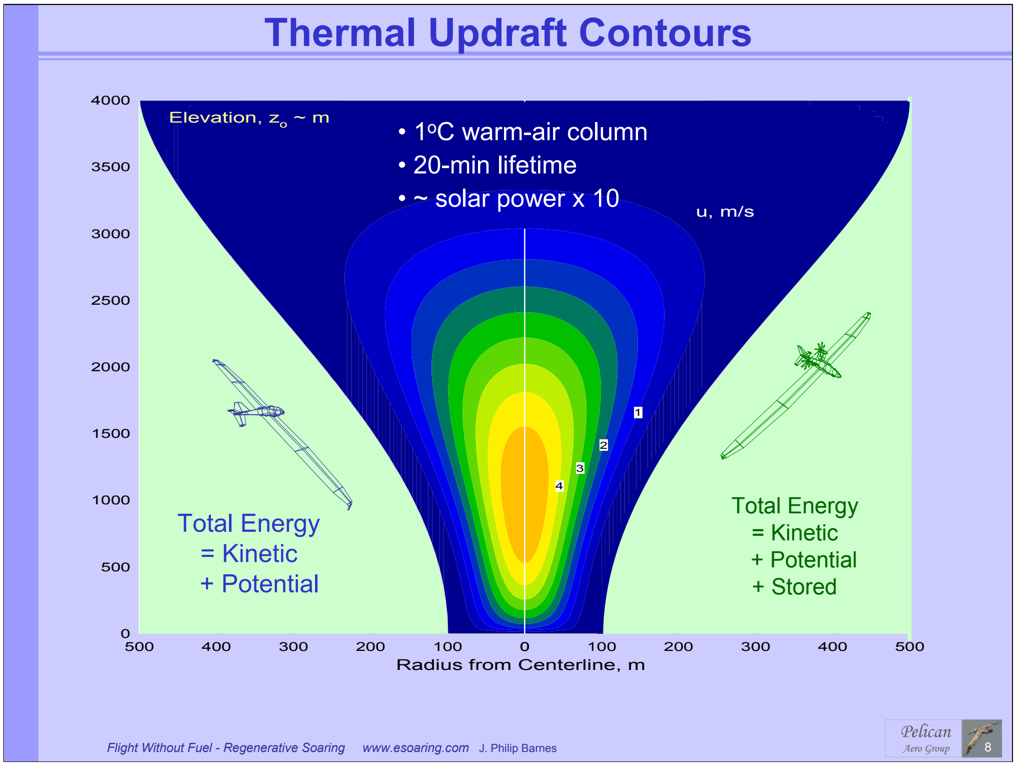

Here is an updraft contour plot for a representative thermal. The diameter is 200-m at the base. The 5-m/s peak-updraft core resides at an elevation of 1000-m. The top of the thermal extends to 4 km elevation with a 1-km diameter, whereupon the updraft velocity falls to zero. We will study the performance of both a sailplane and regen, each operating optimally during the 16-min lifetime of the thermal.

The optimal trajectory for the sailplane will yield the maximum gain in elevation (z_o), whereas for the regen, the optimal trajectory will yield the maximum total specific energy (z_t). As we will show, this means that the best strategy for the regen is to climb more slowly, and gain somewhat less elevation than that of the sailplane.

Presentation Contents

This chart has no footnotes

Weight & Size Impact of Adding Regeneration

265-kg Sailplane
13-m span, A=16

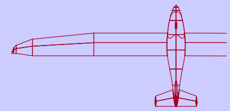

Addition	Weight, kg
Windprop Installation	50
Stored Energy, Takeoff & Climb 1-km	38
Stored Energy, 25-km Cruise	17
Wing Growth	30
Total	135

400-kg Regen
16-m span, A=16

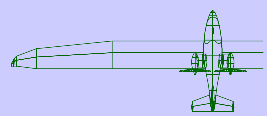

This chart has no footnotes

Sailplane 3-View

- 265 kg
- 13-m
- A=16

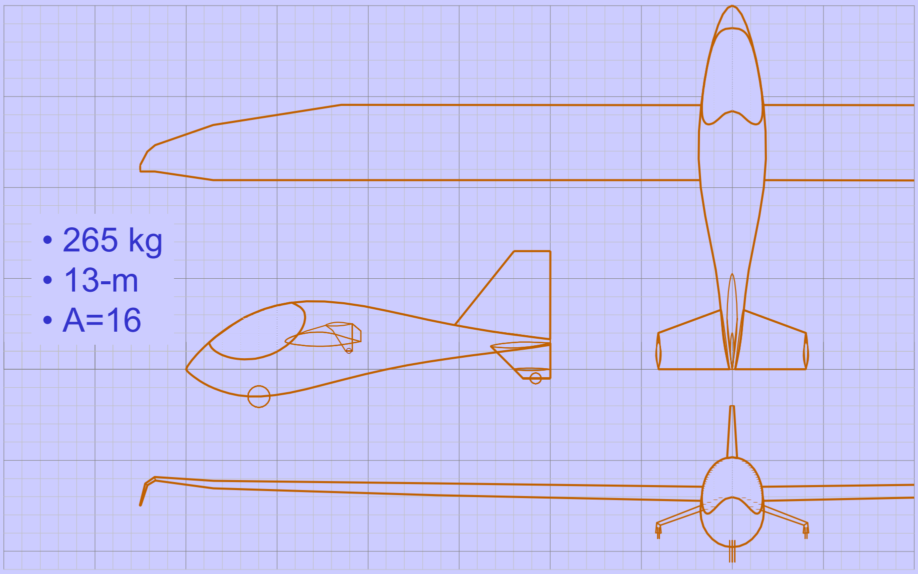

This chart has no footnotes

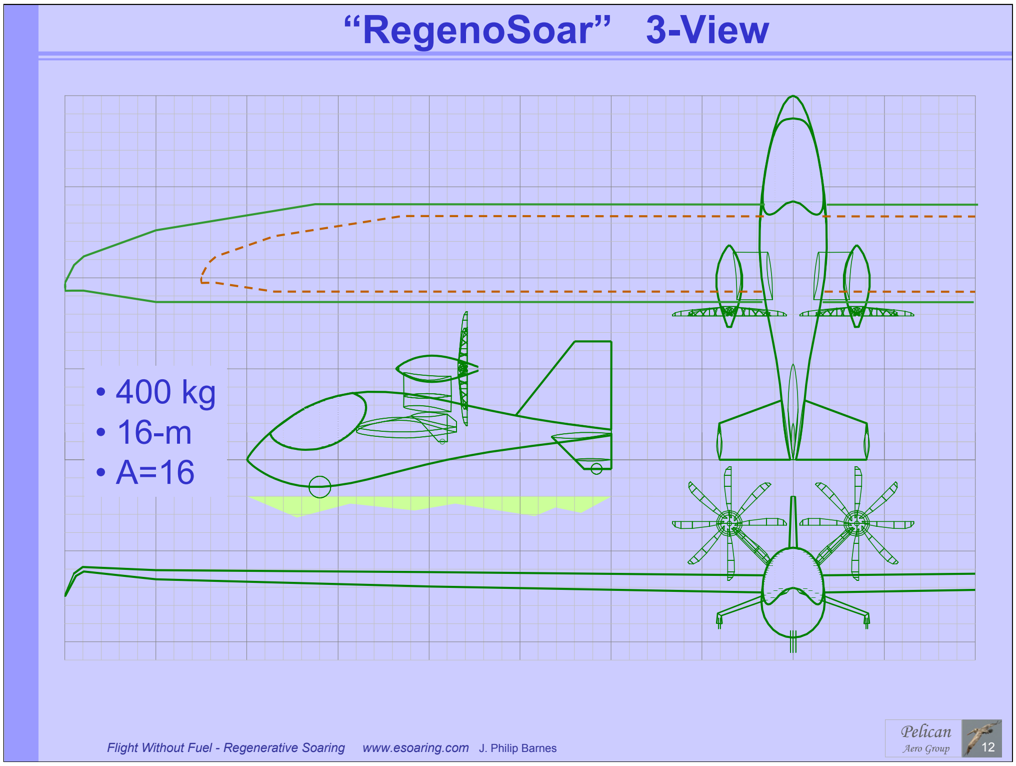

Our rationale for the design of “RegenoSoar” begins with our intent to minimize in-flight aerodynamic interference between the windprops and airframe, while also providing self-contained and robust ground handling by the pilot alone. Thus, the counter-rotating windprops, which allow steering on the ground, are kept aerodynamically clear of the airframe via twin pod installations.

The windprops are arranged in a pusher configuration, whereby the sudden rotational flow imparted by the blades cannot impinge on the leading edges of downstream lifting surfaces which otherwise would suffer interference and induced drag penalties. If necessary, pod-boom trailing-edge blowing may mitigate any adverse affects of the pod-boom wake on windprop operation.

Windprop noise is dramatically reduced via multiple blades operating at high pitch and low rotational speed. The windprop has the smallest diameter which meets requirements for climb thrust and cruise/regen efficiency. The windprop speed control and motor-generator units, housed and air-cooled in the pods, are relatively close to the fuselage-enclosed energy storage unit to minimize line losses and to mitigate aft center-of-gravity trends.

The system enjoys the simplicity of fixed geometry for the windprops and their installation. Retraction or folding mechanisms are not required, and as illustrated later herein, the windprops simply “pinwheel,” with minimal drag penalty, when neither the propeller nor turbine mode is used. A parallel study of a “constant-speed” windprop (actuated blades) yielded 40% greater max-capacity regen power, but did not offer gains in efficiency for any operational mode. Uniform fixed pitch was selected for our study herein.

Finally, the wing design incorporates downward-pointing winglets with integrated tip wheels, the latter required regardless of wingtip configuration. The winglets, which develop aerodynamic thrust in flight, are somewhat elevated above the ground via wingtip dihedral. Such clearance is enhanced as the wing flexes upward under steady lift load. Above a threshold ground-roll speed during takeoff and landing, the empennage and tail wheels will lift off above the ground. Sailplanes characteristically exhibit little or no pitch rotation as they leave the ground in the takeoff tow. Such would also be the case for RegenoSoar during its self-contained takeoff.

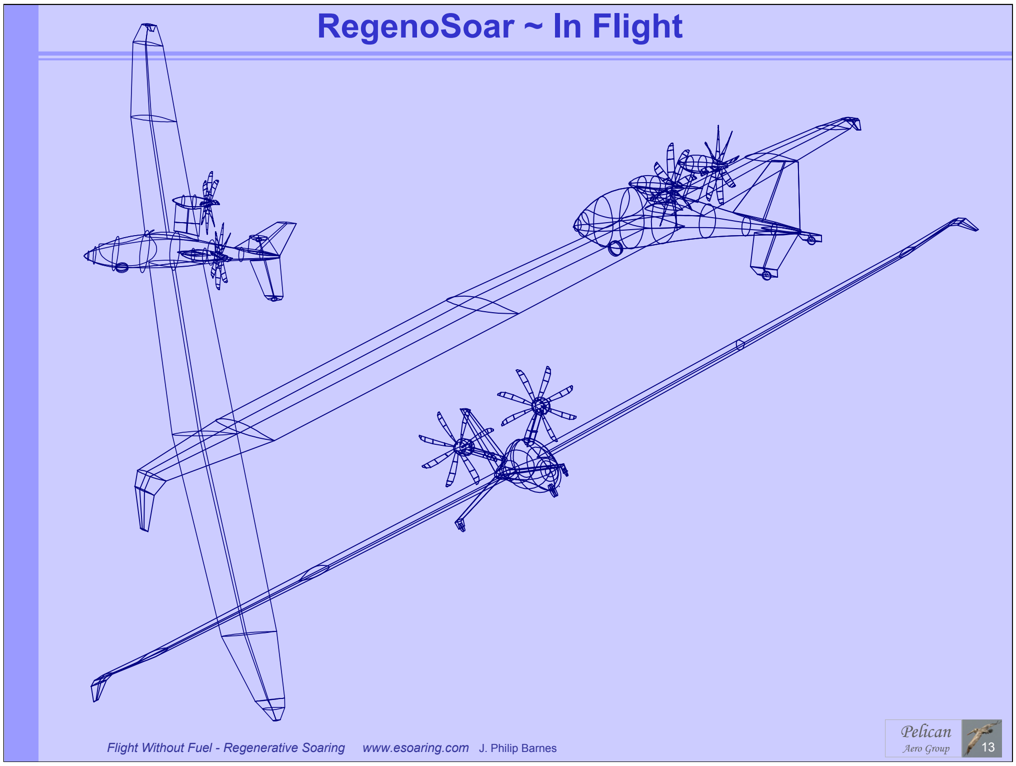

The 3D geometry of “RegenoSoar” is fully characterized with equations. The fuselage, wings, empennage, and windprop blades are modeled as “distorted cylinders.” Canopy-body, wing-body, and windprop blade-spinner intersections are iteratively determined. We show here a wireframe model consisting of a fuselage “prime meridian and equator,” together with section cuts of the fuselage, wing, empennage, and windprop blades, as well as “perimeters” for the wing, empennage, and blades.

An earlier paper by the author introduces methods of mathematically characterizing streamlined shapes. Such characterization reduces drag, promotes sharing of consistent geometry for inter-disciplinary analysis, and takes advantage of today’s precision manufacturing technologies. Interested readers may consult the paper 961317 “Math Modeling of Airfoil Geometry,” available at SAE.org. An analysis of winglet aerodynamic thrust can be found in the author’s paper 975559, “Semi-empirical Vortex Step Method for the Lift and Induced Drag of 2D and 3D Wings.”

Presentation Contents

This chart has no footnotes

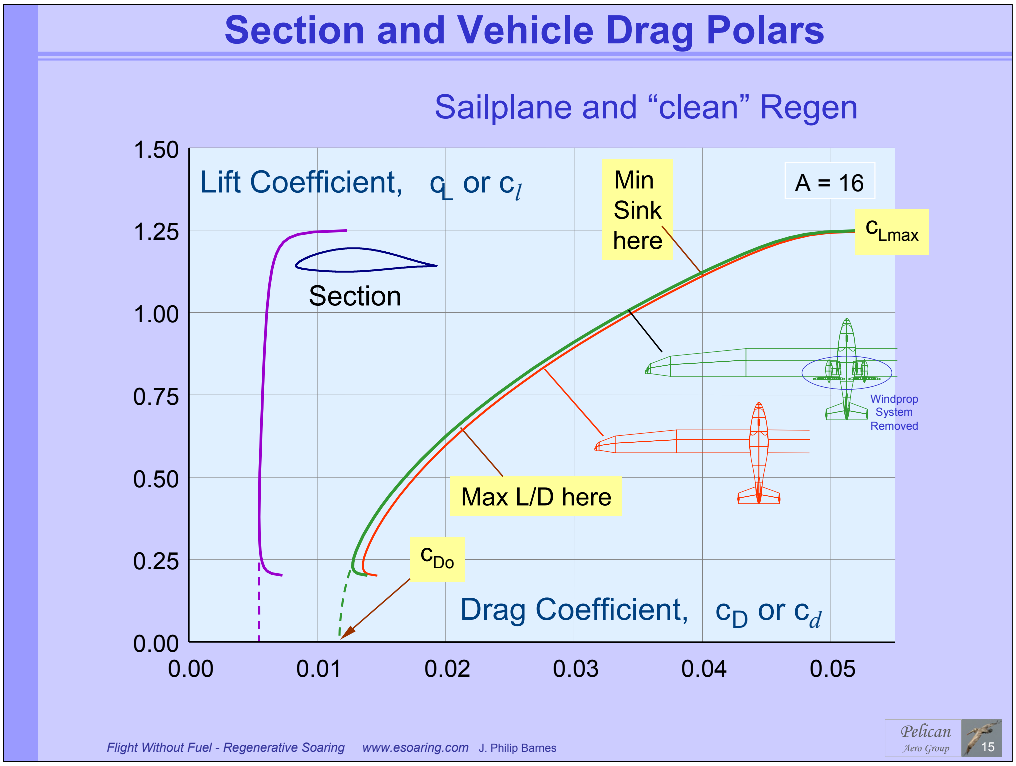

Here we plot the drag polars of both the wing airfoil and total vehicle. Both aircraft (sailplane and "clean" regen) have the same wing loading, and thus the same airspeed. They also share the aspect ratio (A) of 16, thus having similar induced drag, but since also the fuselage and empennage are common, the sailplane zero-lift drag coefficient (c_{Do}) is slightly higher than that of the regen.

Our "thrust-drag accounting" for the regen defines drag to represent the "clean" configuration (windprop system removed), but holding total system weight. All force penalties associated with windprop system addition are treated as thrust penalties, quantified later herein as a non-dimensional drag penalty (Δd/d). For both aircraft, we assume cruise at max L/D and thermalling, with or without regeneration, at minimum sink.

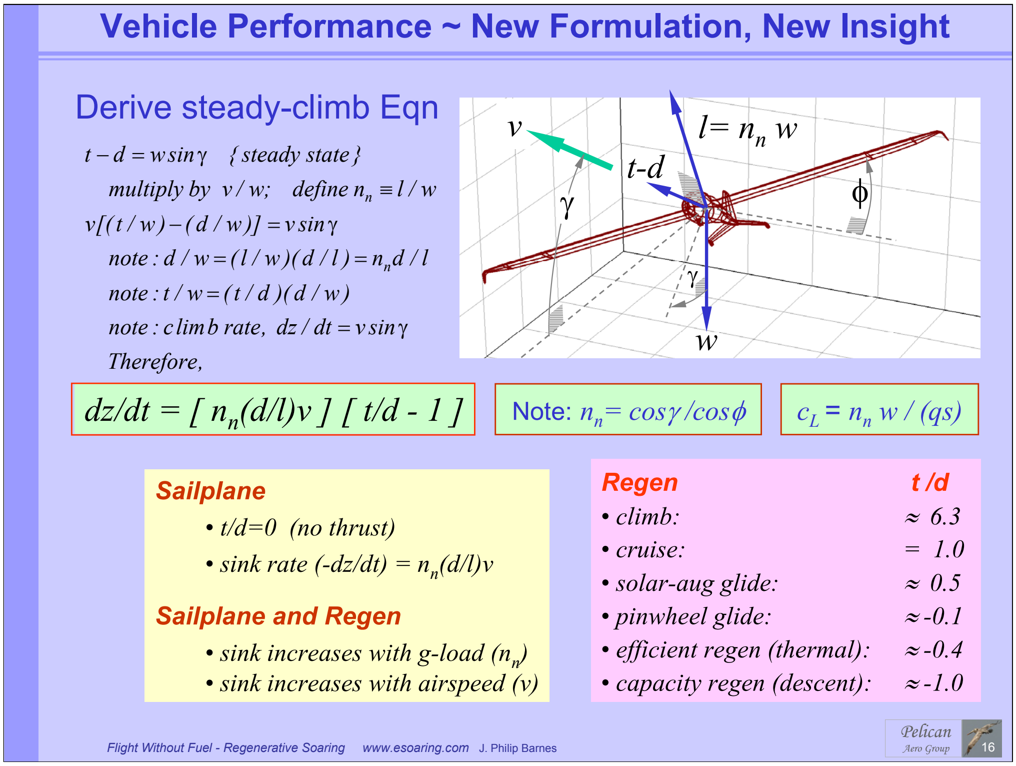

To compare sailplane and regen performance, we must know the climb rate (or sink rate) of the maneuvering aircraft, taken relative to the local airmass. In particular, we are interested in the effects of g-load, or normal load factor (n_n), lift-to-drag ratio (l/d), and thrust-to-drag ratio (t/d). Our diagram and analysis together describe the effects of the forces acting on the aircraft climbing at a flight path angle (γ) and banked at the angle (ϕ). The lift vector (l), normal to the airspeed vector (v), has the value ($n_n w$), where (w) designates weight. Note that flight path angle (γ) will be negative if the aircraft is sinking in relation to the surrounding airmass.

After "normalizing" the various forces in terms of dimensionless ratios, we find that the steady-state climb rate (dz/dt), whether in still air or as seen by a balloon-based observer rising with the thermal, is given by the product of an "aerodynamic group" [$n_n(d/l)v$] and a "propulsive group" [(t/d)-1]. Indeed, the aerodynamic group is the *sink rate* in still air with the propulsion system "aerodynamically removed." For the sailplane (t/d=0), climb rate is of course negative. For either the sailplane or "clean" regen, sink or climb performance is degraded as load factor (n_n) is increased, with (l/d) evaluated at the lift coefficient under load. Thus, turning "twice increases" the drag penalty, and this leads to high aspect ratio (as we learn from the albatross!) to mitigate this effect.

For the regen, climb rate depends on the "clean sink rate" for the chosen airspeed, and the propulsive group. The latter will be positive for climb, zero for cruise (dz/dt=0), and negative during regen. As expected, the regen sinks faster when the windprop operates as a turbine. In the glide between thermals, the windprop pinwheels with a small drag penalty (t/d<0).

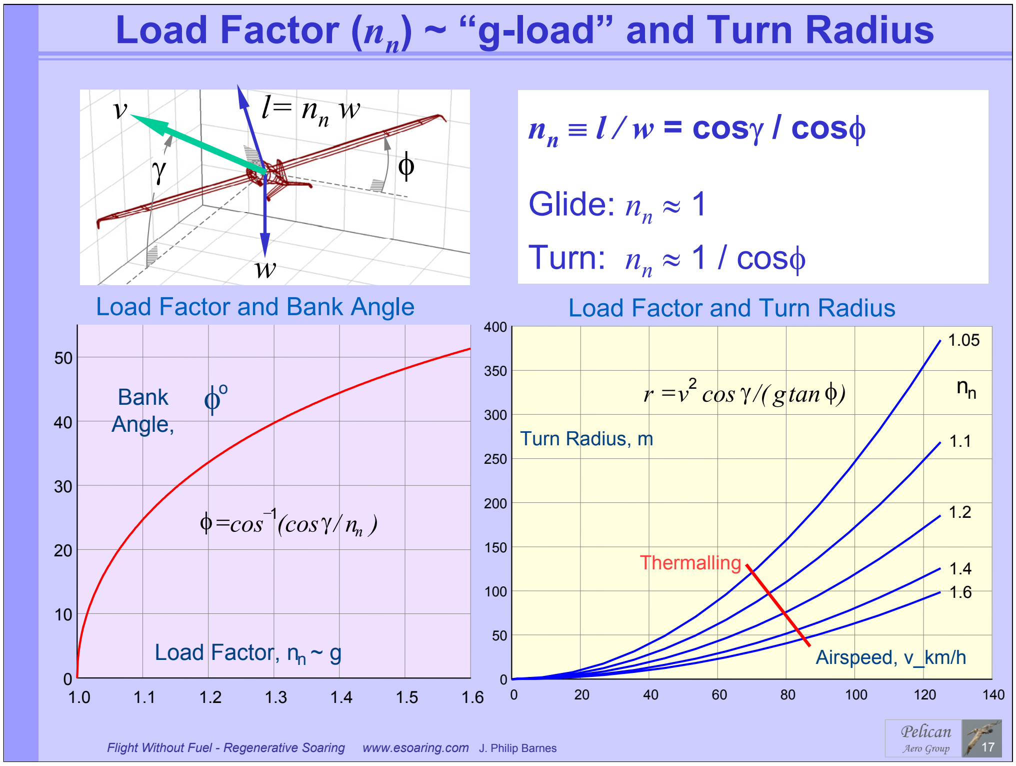

In a wings-level glide, the load factor (again, n_n is defined as lift/weight) is essentially unity (actually "cos γ"). With turning, the load factor will be greater than unity, and it has a unique bank angle, for example 40-deg at n_n=1.3 (or "1.3-g"). Together with airspeed, the load factor determines the turn radius (r), for example 250-m at 100 km/h and 1.05-g. All of these results apply to any aircraft with flight conditions whereby cosγ is near unity (most subsonic aircraft).

The red line at lower right indicates the locus of minimum-sink, an essential performance characteristic for any sailplane (or regen). Let's next determine how to show where that line resides.

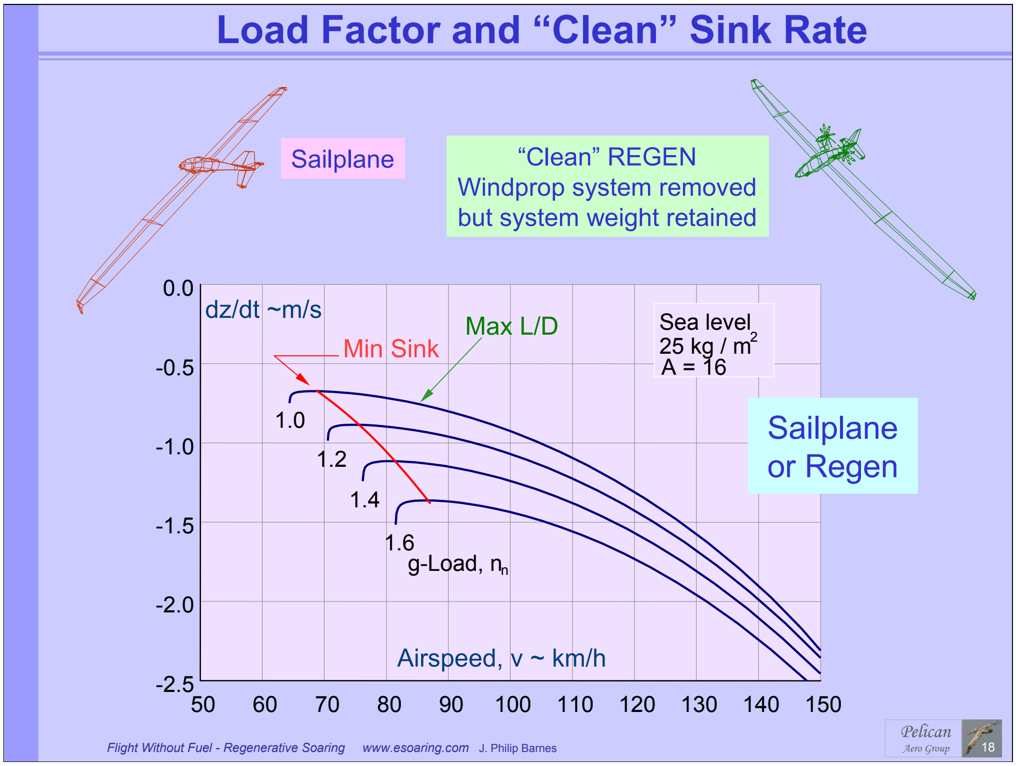

To relate the normal load factor (n_n) to sink rate and airspeed, we first recognize that the lift coefficient (c_L) includes the load factor as shown in the formula at the upper right. The drag polar then provides the drag coefficient, and the ratio of drag-to-lift (*D/L or d/l*)* is then equal to the ratio of drag-to-lift coefficients (c_D/c_L).

Now we can calculate the still-air clean sink rate, [$n_n(d/l)v$], the latter clearly proportional to load factor. For example, the aircraft in max L/D glide (1.0-g) sinks at 0.75 m/s at 85 km/h airspeed. However, the aircraft turning at 1.4-g sinks at 1.25-m/s at 100 km/r airspeed. The left-hand tip of each curve represents operation at max lift coefficient, and the maximum of each curve represents minimum-sink operation.

Finally, we note that the graph above shows the "clean sink rate." When the windprop system is added, operating in the turbine mode, the regen aircraft will fall more quickly through the thermal. We will calculate the sink rate during regeneration later herein.

* Note on notation:

Most of our charts and notes herein implement a suggested nomenclature philosophy using lower-case letters to represent dimensional variables, and upper-case letters to represent dimensionless groups thereof. For example, lift and drag would become (*l,d*), and their corresponding coefficients would become (*L,D*). Until such may be implemented, we retain c_L, c_D.   Either way, c_L/c_D = L/D.

Presentation Contents

This chart has no footnotes

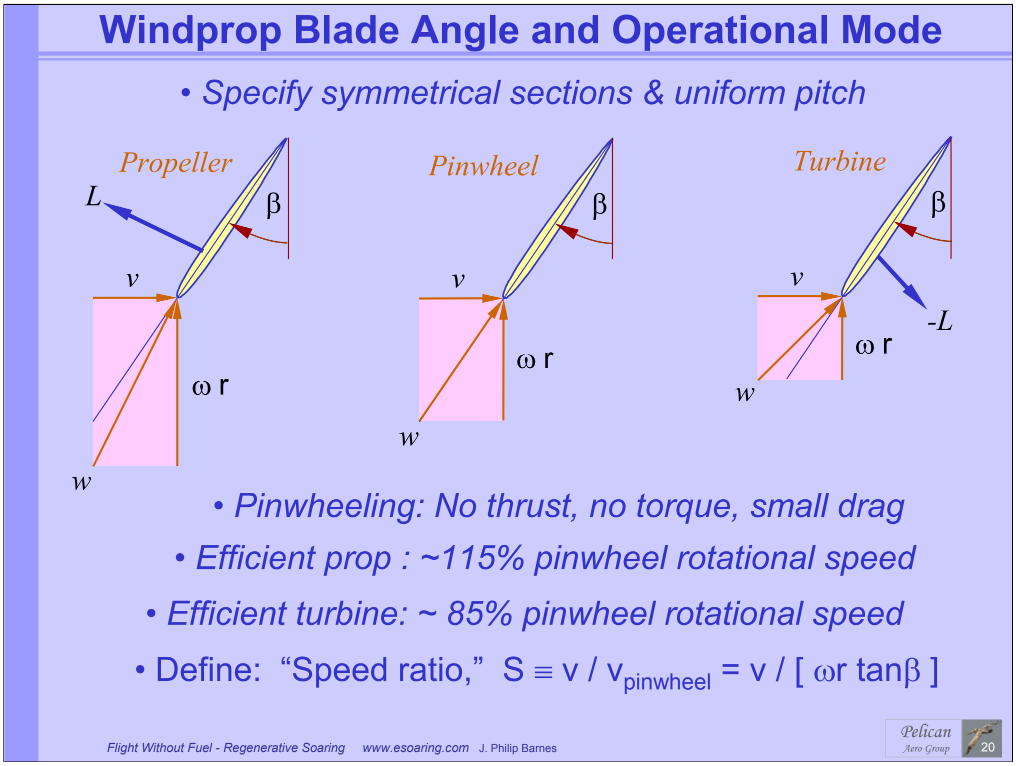

Here we show a section of the windprop blade at the angle (β) from the plane of rotation. The blade relative wind (w) represents the vector combination of the airspeed (v) and rotational velocity (ω r). For the diagram representing pinwheeling, the blade section has zero angle of attack(α) since the relative wind vector (**w**) is aligned with the chord. If we now increase the rotational speed while holding constant airspeed, the blade will develop lift, thrust, and torque as a propeller. Conversely, if we reduce rotational speed, the blade will develop negative values thereof, thus acting as a turbine. Alternatively, we can imagine holding fixed rotational speed as flight velocity varies.

We are thus led to the definition of a new term, or "speed ratio" (S), which applies to both propeller and turbine operation, while also highlighting the pinwheeling regime which separates these two power-exchange modes. We define (S) as the ratio of flight velocity to the "pinwheeling" flight velocity where, for the stated pitch and rotational speed, windprop thrust in propeller mode would fall to zero. Any subsequent increase of airspeed (S>1) would yield turbine operation. A speed ratio of zero represents ground static propeller-mode operation, where thrust and torque coefficients must include the effects of stalled blades. Although the speed ratio (S) enjoys some similarity to the more familiar "advance ratio" (J), only the former describes at once the essential relationship of the three conditions represented by propeller, pinwheel, and turbine operation.

Note that the relative wind vector (w) is shorter for the turbine mode. Local forces vary with (w^2), while shaft power varies roughly with the cube of rotational speed (ω). Thus, turbine operation is significantly "power limited" in relation to propeller operation. As we shall learn, this limitation fundamentally affects how the regen flies in the thermal.

Windprop Wake and Blade Loading

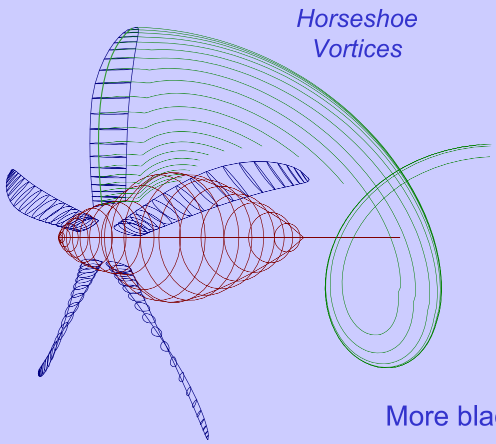

- Pitch:
  helix length per rotation
  $h_{tip} = 2\,\pi\,R \tan \beta_{tip}$
- Uniform pitch:
  $r \, tan\, \beta = R \, tan\, \beta_{tip}$
- Blade tip angle (β_{tip}):
  14^o ~ low pitch
  30^o ~ high pitch

More blades at fixed thrust & diameter:

- More wakes (one per blade)
- Higher pitch ~ wakes farther aft / rotation
- Lower rotational speed, lower tip Mach
- Upshot: ~ similar efficiency, 2 to 8 blades

As shown in this figure, each blade sheds a helical wake. We can calculate the wake-induced velocities and blade loading with a vector integration using the horseshoe vortices arranged along each blade. This method, documented in our technical paper “Math Modeling of Propeller Geometry and Aerodynamics,” has been used to compute the fixed-geometry windprop performance which we describe next.

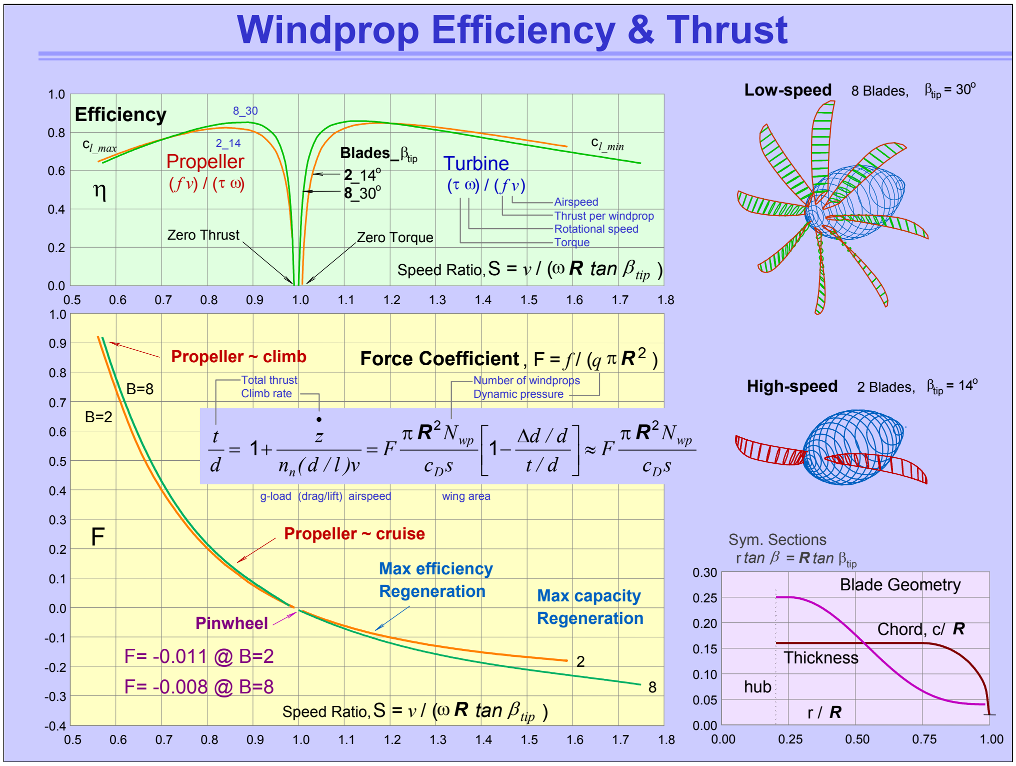

Here we plot windprop efficiency versus the “speed ratio” (S) for two fixed-geometry, uniform-pitch windprop designs sharing the same diameter and climb thrust. The high-RPM option has two blades with 14-deg blade tip angle, and the low-RPM design has eight blades with 30-deg blade tip angle. In either case, propeller efficiency has the traditional definition with shaft power in the denominator, whereas turbine efficiency follows Glauert’s definition for an airborne turbine, with shaft power in the numerator. Since for turbine operation both torque and force change sign, turbine efficiency remains positive. Note also that turbine efficiency is not subject to the “Betz Limit” of a ground-based wind turbine which uses a different definition of efficiency.

As noted earlier, the speed ratio (S) is defined as the ratio of flight velocity to “pinwheel flight velocity,” where thrust and torque fall to zero with the windprop operating as a propeller at a stated rotational speed. Windprop efficiency is zero in the pinwheel regime ($S \approx 1$). At speed ratios above unity, the windprop operates as a turbine. For both propeller and turbine operating modes, the curves above terminate at the first appearance, anywhere along the blade, of blade section maximum lift coefficient (c_{l_max}).

Finally, we plot the force coefficient (F), again versus speed ratio (S). This force coefficient is referenced to windprop disk area and flight dynamic pressure (q). Such characterization, together with the formula in the blue box, allows us to easily relate installed thrust-to-drag ratio (t/d), aircraft drag coefficient (c_D), wing area (s), windprop radius (R), number of windprops (N_{wp}), and climb rate (dz/dt). Regardless of operational mode, installed thrust (t) includes the normalized change in drag ($\Delta d/d$) due to windprop system addition.

Interim Summary ~ Windprop Aerodynamics

- Comparable *installed* efficiencies for:
  - 8-blade low-speed, high-pitch, with gearbox
  - 2-blade high-speed, low-pitch, w/o gearbox
- 8-blade windprop has the edge overall:
  - 25% less pinwheel drag (@ S ~ 1.0, zero torque)
  - 35% more max-capacity regen (@ S ~ 1.75)
  - Quiet operation and reduced tip Mach number
- Windmilling is “power limited” vs. propeller oper.
  - Turbine operation decelerates captured streamtube
  - Increasing regen reduces rotation speed & power

This chart has no footnotes

Presentation Contents

This chart has no footnotes

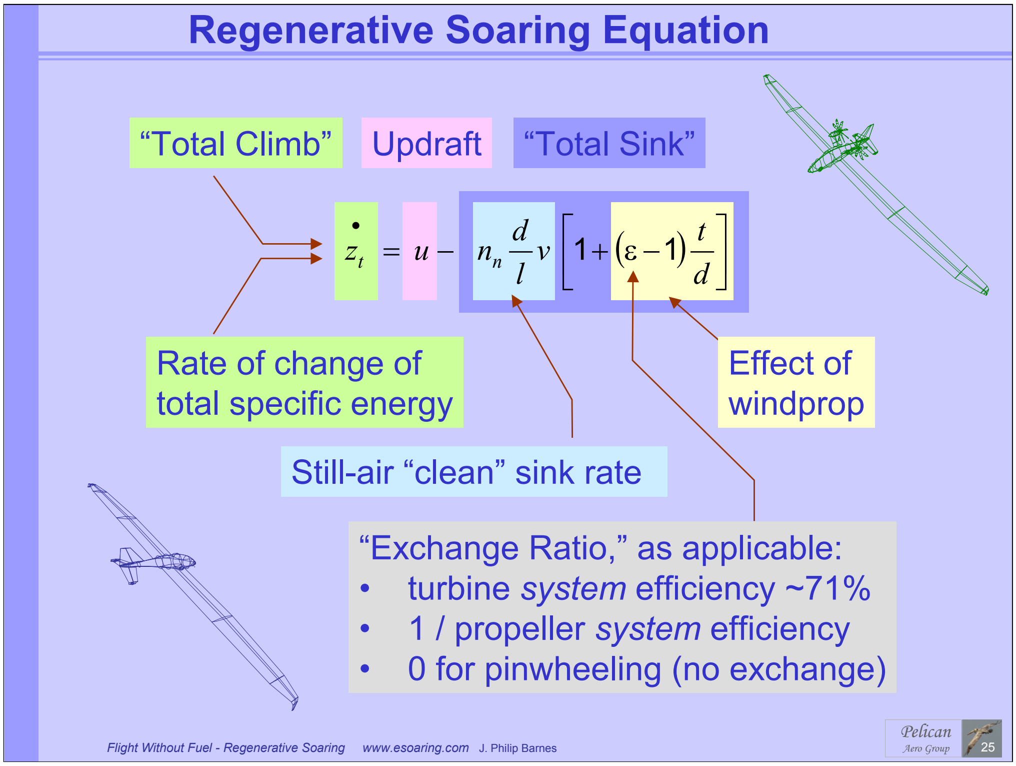

A key product of our study is a fundamental "Regenerative Soaring Equation" (RSE) relating the total climb rate to the updraft and total sink rate. Interested readers can consult the technical paper "Flight Without Fuel," for its derivation. Whereas the updraft provides the specific power into the system, the total sink term represents the specific power lost to both aerodynamic drag and windprop operation.

The RSE is generally applicable to both a sailplane (where t/d=0) and a regen in any operating mode. The "exchange ratio" (ε), determined by operating mode, is set to zero if the regen is pinwheeling, whereby the system "exchanges" no shaft power, and whereby the term (t/d, about -0.10) represents pinwheeling thrust (negative) as a fraction of aircraft drag. Otherwise, the exchange ratio is set to turbine *system* efficiency or the inverse of propeller *system* efficiency, whichever is applicable. Recall that thrust is negative in the turbine mode.

Application of the Regenerative Soaring Equation

Item / mode --->	**Climb** max L/D	**Cruise** max L/D	**Pinwheel** max L/D	**Regen** max efficiency, minimum sink, z_o=1480-m	**Regen** max capacity, minimum sink, z_o=1480-m
Airspeed, v ~ km/hr	85.0	85.0	85.0	77.2	77.2
Updraft, u ~ m/s	**0.00**	**0.00**	**0.00**	**3.72**	**3.72**
Turn radius, r ~ m	n/a	n/a	n/a	56.5	56.5
Load factor, n ~ g	1.00	1.00	1.00	1.30	1.30
Lift coefficient, c_L	0.64	0.64	0.64	1.12	1.12
Drag coefficient, c_D (clean)	0.022	0.022	0.022	0.040	0.040
Installed thrust/drag ratio, t/d	**6.33**	**1.00**	**-0.10**	**-0.40**	**-1.01**
Installation penalty, $\Delta d/d = -\Delta t/d$	0.17	0.09	0.10	-0.03	-0.03
Clean sink rate, still air, $n(d/l)v$ ~ m/s	0.75	0.75	0.75	1.03	1.03
Climb rate in still-air, dz/dt ~ m/s	4.00	0.00	-0.83	-1.43	-2.06
Total energy rate, dz_t/dt ~ m/s	**-5.40**	**-1.05**	**-0.83**	**2.58**	**2.18**
Ground-observed climb, dz_o/dt ~ m/s	4.00	0.00	-0.83	2.29	1.66
Windprop speed ratio, S	0.57	0.85	1.00	1.15	1.75
Windprop speed ~ RPM	**1096**	**735**	**625**	**494**	**324**
Force group, F	0.92	0.14	-0.0070	-0.10	-0.26
Windprop efficiency, η_t or η_p	0.63	0.84	n/a	0.85	0.64
Powertrain efficiency (non-windprop)	0.80	0.85	n/a	0.85	0.8
System efficiency η_{st} or η_{sp}	**0.50**	**0.71**	**n/a**	**0.72**	**0.51**
Exch. ratio, $\varepsilon = 1/\eta_{sp} : \eta_{st} : 0$ (applic.)	1.98	1.40	0.0	0.72	0.51
Total Shaft power, $\tau\omega$ ~ kW	29.5	3.50	0.00	-1.36	-2.58
Energy storage rate ~ kW	**-36.9**	**-4.12**	**0.00**	**1.16**	**2.07**

Here we apply the ***Regenerative Soaring Equation*** (and related formulas) to compute the performance parameters of the regen in each of its operating modes. The table shows the various rates ($dz\_/dt$) with applicable sign conventions. Table entries at lower left show how the propeller climb mode exercises system capacity.

Notice that thrust/drag ratio (t/d) is 6.33 in climb, but is -1.01 for max-capacity regen as the aircraft turns at 1.3-g with the windprop spinning at a relatively-slow 324 RPM. For this example, the max-capacity regen condition can be interpreted as having the drag doubled by windprop operation.

After takeoff, the aircraft climbs in still air at (dz/dt = 4.00 m/s) as total specific energy (kinetic, potential, & stored) decreases (dz_t/dt = - 5.40 m/s). Once the regen is well into the thermal and regenerating, say at max capacity, a balloon-based observer rising with the updraft at 3.72 m/s sees the aircraft falling (dz/dt = - 2.06 m/s). At the same time, a ground-based observer sees the aircraft climbing (dz_o/dt = 1.66 m/s).

Although we include max-capacity regen here for study purposes, only max-efficiency regen has competitive flight performance. Note that total specific energy increases more rapidly with max-efficiency regen than with max-capacity regen. However, regen at max-capacity proves useful in many scenarios, including final descent for landing where, for this example, the energy storage rate is 2.07 kW. Indeed, if the last-encountered updraft is near the airport, landing on a full charge can be routine.

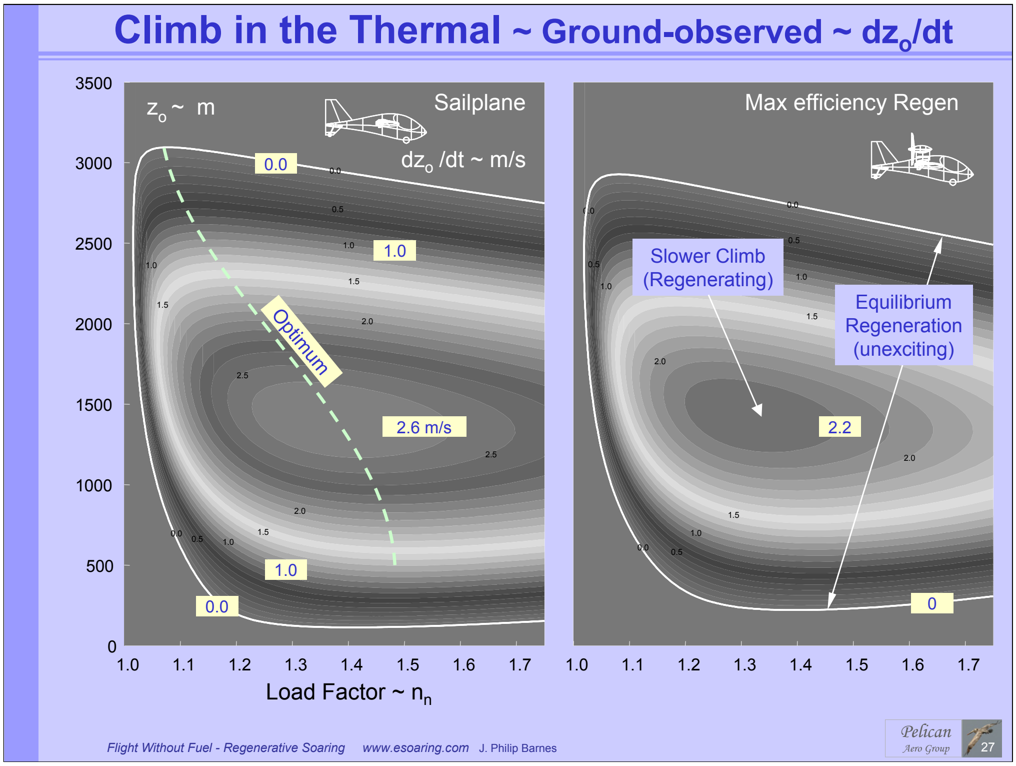

Here we have applied the foregoing models and methods to calculate and plot, versus load factor and elevation, contours of ground-observed climb rate (dz_o/dt) in the thermal, for both the sailplane and regen. The sailplane obtains a maximum climb rate of 2.6 m/s turning at 1.4-g around 1500-m elevation. The regen, shown at the right, climbs more slowly because it is storing energy during the climb.

We will assume that for both aircraft, the interesting part of the thermal extends from 500-m to 2500-m elevation. The dashed curve represents the optimum (minimum time-to-climb) “trajectory” in terms of load factor versus elevation, indicating tight, 1.5-g turns at low level but wider, 1.1-g turns near the top of the thermal.

The white contour for each aircraft represents flight at fixed elevation. The regen could undertake “equilibrium regeneration” at either 200-m or 2700-m, but at those elevations the thermal has little to offer. Thus for the most effective strategy, *the regen climbs in the thermal as it regenerates*. This is a fundamental result, not anticipated at the outset of our study where we had anticipated equilibrium regeneration would be a typical operational mode.

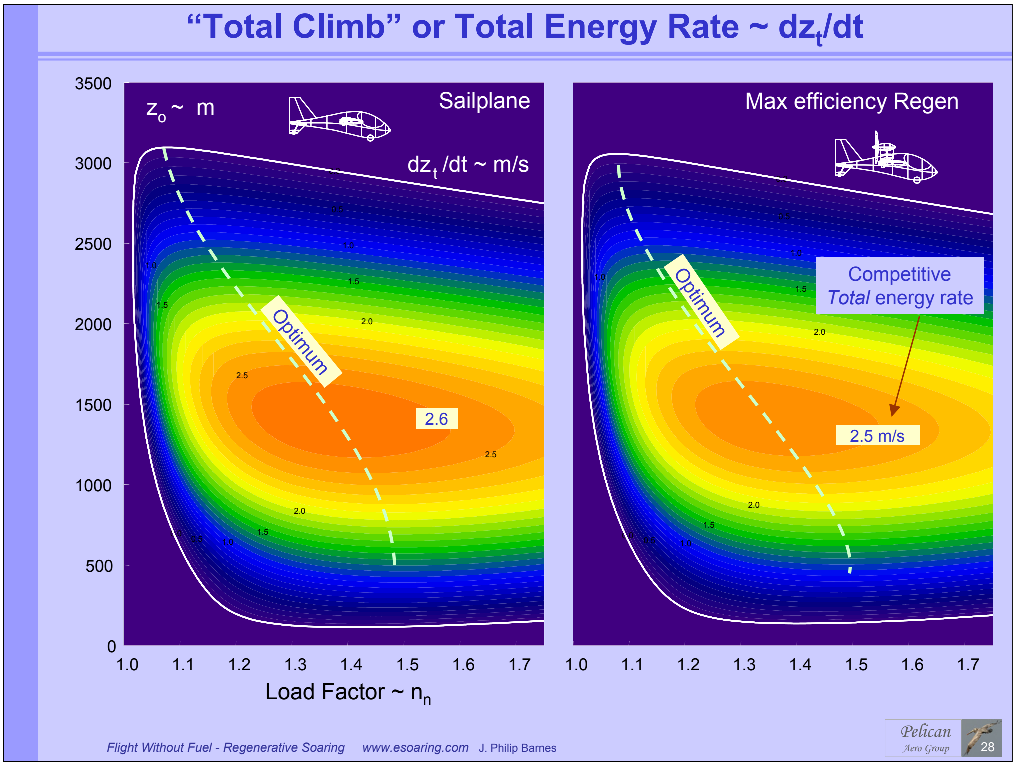

Next we plot the total climb rate, or rate of change of total specific energy. For the sailplane (where $dz_o/dt = dz_t/dt$), this is the same data as just shown, but with different colors. But for the regen, the rates “dz_o/dt” and “dz_t/dt” are distinct due to the energy storage feature.

Note that the regen gains total specific energy at almost the same rate as the sailplane. The peak rate, along the optimal total-energy “trajectory” represented by the combination of load factor and altitude, is about 2.6 m/s at 1500-m.

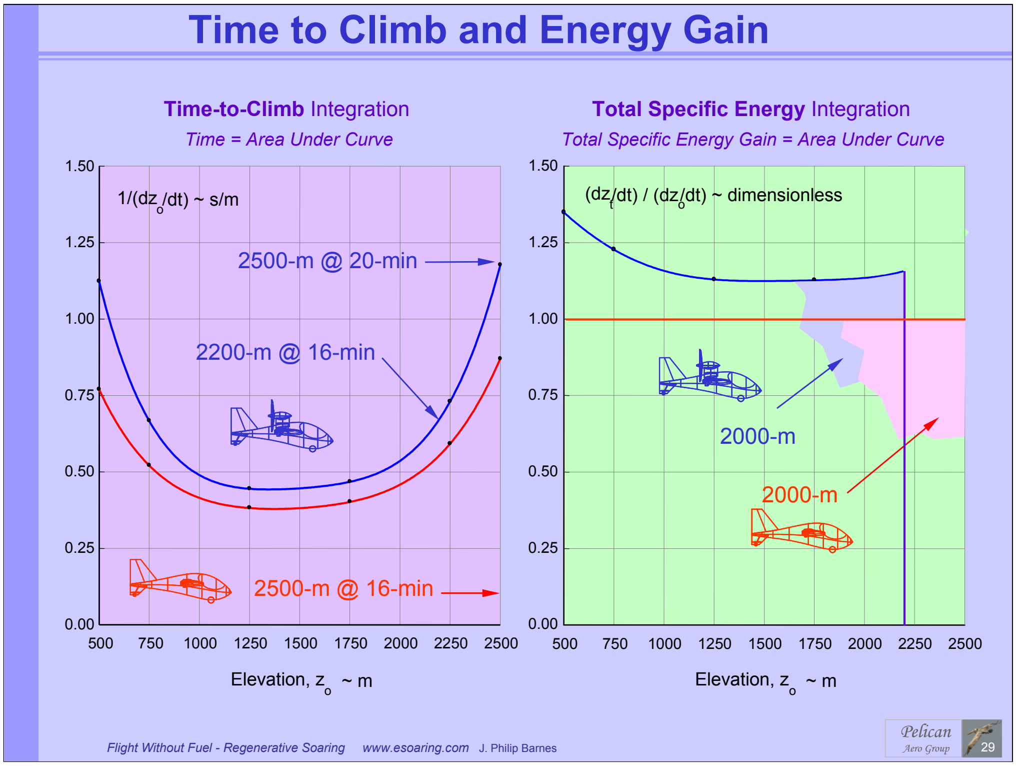

Following the previously-described load-factor trajectories, the time to climb is obtained by taking the area under the curve of the inverse of climb rate versus elevation. The sailplane makes the climb in 16-min, but the regen takes 20-min, thus exceeding the 16-min limit we had established with the intent of avoiding early disappearance of the thermal.

Therefore, in integrating the total energy (see the right-hand figure), both aircraft stay within the 16-min limit, whereby the regen terminates its climb at 2200-m. Nevertheless, the areas are similar, indicating total specific energy gain of 2000-m for either aircraft. Whereas the sailplane gains 2000-m of elevation, the regen gains 1700-m elevation, plus 300-m of stored specific energy. Having “earned” the latter, the regen can immediately “spend it” with a short level cruise. As we shall see next, this yields an interesting advantage for the regen.

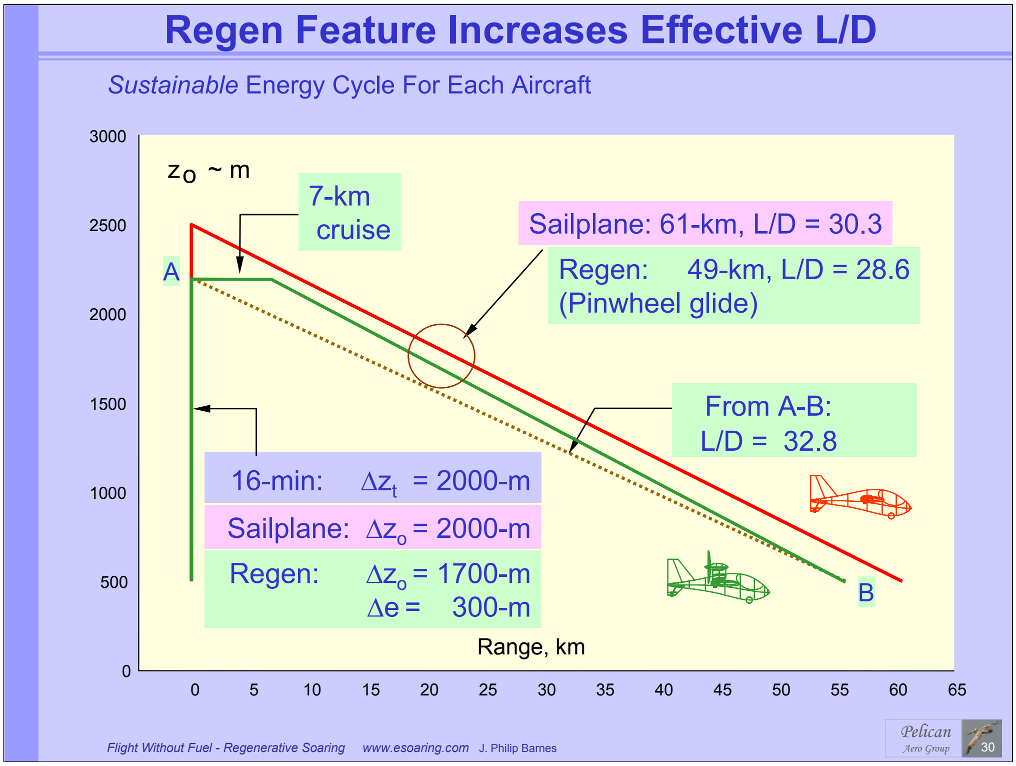

Finally, we plot the 2D flight trajectories and energy cycles for each aircraft. At range zero, where the thermal resides, the sailplane thermals up from 500-m to 2500-m, whereas the regen thermals up to 2200-m. However, both aircraft gain 2000-m of total specific energy, of which 300-m has been stored by the regen. Whereas the sailplane then glides 61-km to the next thermal, the regen first operates the propeller for a 7-km level cruise, thus "spending" the energy it has "earned" in the thermal, and then glides 49-km with the windprop pinwheeling.

We find that for our sustainable "energy budget" under study, the range of the regen falls about 8% short of that for the sailplane. However, most interestingly, the effective L/D of the regen is 8% higher than that of the sailplane when we recognize that the regen travels ultimately from A to B in each sustainable energy cycle, without consuming any stored energy.

Overall, no matter how we interpret these results, or perhaps change the groundrules and repeat the study, we will find the regen to exhibit competitive performance with the sailplane, while adding the regen-unique capabilities of self-contained takeoff and emergency cruise or climb.

Presentation Contents

This chart has no footnotes

Preview ~ Solar-Augmented Regenerative Soaring

- Add solar panels to perhaps 75% of wing area
- Solar package delivers ~150 W/m^2_panel
  - Not intended to *sustain* level flight for regen herein
    - Thus “solar-augmented,” not “solar-powered”
- Solar-augmented glide between thermals
  - Adds thrust (vs. small drag penalty of pinwheeling)
  - Operate in propeller mode at about half of level-flight thrust
  - Significantly *enhanced effective L/D* during glide
  - Sustainable: powered glide consumes no stored energy
- Solar feature promotes “landing on a full charge”
- Solar feature resolves “loss of charge” on the ground

This chart has no footnotes

Conclusions ~ Flight Without Fuel

- Windprop: comparable & good efficiency in either mode
- Regen flight *emulates* that of a sailplane
  - Regen climbs in the thermal during regeneration
  - "Earn & spend" short cruise; pinwheel glide to next thermal
- Regenerative soaring is *sustainable*
  - Stored energy is *reserved* for emergency cruise/climb
- Regen soaring is *competitive* with classical soaring
  - Regen loses 8% range compared to sailplane, but:
  - Regen exhibits 8% higher effective L/D than sailplane
  - Additional regen-unique strategies yet to be discovered
- Solar augmentation adds significant benefits
- Theory says thumbs up ; Now let's build and fly!

This chart has no footnotes

About the Author

Phil Barnes has a Master's Degree in Aerospace Engineering from Cal Poly Pomona and a Bachelor's Degree in Mechanical Engineering from the University of Arizona. He has 25-years of experience in the performance analysis and computer modeling of aerospace vehicles and subsystems at Northrop Grumman. Phil has authored technical papers on aerodynamics, gears, and flight mechanics. Drawing from his SAE technical paper of similar title, this presentation brings together Phil's knowledge of aerodynamics, flight mechanics, geometry math modeling, and computer graphics with a passion for all types of soaring flight.

This chart has no footnotes